CONF-850871--10

# STRUCTURAL PHASE TRANSITION IN $CeCu_6$*

by

M. L. Vrtis,** J. D. Jorgensen, and D. G. Hinks
Materials Science and Technology Division
ARGONNE NATIONAL LABORATORY
Argonne, Illinois 60439

and

**Department of Physics and Astronomy
Northwestern University
Evanston, IL 60201

CONF-850871--10

DE85 018362

August 1985



## DISCLAIMER

rt



To be Submitted to the International Conference on Neutron Scattering, Santa Fe, NM, August 19-23, 1985.



*Work supported by the U. S. Department of Energy, BES-Materials Sciences, under Contract W-31-109-Eng-38.

# STRUCTURAL PHASE TRANSITION IN $CeCu_6$*

M. L. Vrtis,** J. D. Jorgensen, and D. G. Hinks
Materials Science and Technology Division
Argonne National Laboratory
Argonne, Illinois 60439

and

**Department of Physics and Astronomy
Northwestern University
Evanston, Illinois 60201

## ABSTRACT

The structure of $CeCu_6$ has been studied at eight temperatures from 10K to 295K by time-of-flight neutron powder diffraction. The high temperature orthorhombic cell transforms to a monoclinic cell at 230K. Rietveld structural refinements at each temperature give details of the structural distortion associated with the transition. The space groups and the temperature dependence of the monoclinic strain are consistent with a second order transition driven by a soft acoustic phonon mode. However, small atom displacements perpendicular to the shear direction suggest that an optic mode may also be involved in the transition.

*Work supported by the U.S. Department of Energy, BES-Materials Sciences, under contract W-31-109-Eng-38.

The recent discovery that the intermetallic compound $CeCu_6$ exhibits a large low-temperature specific heat $\gamma$ (i.e., heavy fermion behavior)[1] has generated much interest in the characterization of the material. In addition to the specific heat measurements, the literature reports the anisotropic magnetic and electrical properties on single crystal specimens[2] and nuclear magnetic resonance studies.[3]

The interest in the various properties of this material is primarily at low temperature where the Kondo-like behavior of the cerium ions become evident. Previous work has assumed (incorrectly) that the low temperature structure of $CeCu_6$ is the same as at room temperature, i.e., orthorhombic Pnma.[4] The purpose of this work was to determine the structure of $CeCu_6$ at low temperature. Powder neutron diffraction data show that the structure is monoclinic below about 230K.

The sample was obtained from an ingot of $CeCu_6$. The single-crystal ingot was pulled from an inductively-heated melt contained in a tungsten crucible. The sample was then crushed into a fine powder and approximately 25 gms was sealed in a vanadium can with 1 atm of helium exchange gas.

Neutron diffraction measurements were performed on the Special Environment Powder Diffractometer (SEPD) at Argonne's Intense Pulsed Neutron Source[5] with the sample cooled by a Displex (Air Products and Chemicals, Inc.) closed cycle helium refrigerator. Data were collected for about four hours at each of eight temperatures starting at 10K and ending at 295K.

The 295K and 250K data were analyzed by the Rietveld technique[6] in the orthorhombic Pnma space group with initial atomic positions and lattice constants obtained from the work of Cromer and Larson.[4] The refined parameters agreed well with those in the literature.[4,7]

At 200K and lower temperatures, the data could not be refined with the Pnma orthorhombic model. The observed gradual splitting of the Bragg peaks suggested a continuous transition to a lower symmetry structure. The monoclinic space group

$P2_1/c$ (a subgroup of Pnma) agreed with the observed extinctions and was, thus, used to refine the data for 200K - 10K. A plot of the raw data and the calculated Rietveld profile at 10K is shown in Fig. 1.

The refinement in the orthorhombic phase included 713 allowed reflections with d-spacings from 0.69 Å to 2.66 Å. In the monoclinic phase, the total number of allowed reflections increased to 1281 for nominally the same data range. Table I lists the lattice parameters at each temperature. Table II gives full structural parameters at 295K and 10K. (Parameters for the other temperatures can be obtained from the authors.) Both structures are described in standard settings, which introduces a permutation of axes when going from the orthorhombic to the monoclinic cell.

Within the precision of this measurement, the lattice parameters and the unit cell volume show smooth changes versus temperature, supporting the hypothesis of a continuous transition. Landau theory allows the transition from Pnma to $P2_1/c$ to be second order with a proper order parameter being the monoclinic strain $ac\cos\beta$. Fig. 2 shows a plot of $(ac\cos\beta)^2$ versus temperature. The data fall on a straight line, indicating that the transition temperature (by extrapolation of the least-squares-fit straight line is 230K, and that the transition can be adequately modeled by mean field theory with an exponent of 1/2. Without an independent measurement of the transition temperature or a careful search for hysteresis, however, it is impossible to conclude from this work whether the transition is actually second order.

The atom motions associated with the transition can be described predominantly as a shear with some atoms exhibiting a small amount of displacement perpendicular to the shear direction. As shown in Table II, all atoms except Cu1 lie in planes at y = 1/4 and 3/4 in the orthorhomic structure. The shear is along the orthorhombic a axis, parallel to these planes. Displacements perpendicular to the planes are largest for one of the copper atoms, Cu4, which has a short Ce-Cu distance. (Fig. 3)

Since this displacement of Cu4 perpendicular to the shear direction is not consistent with the transverse acoustic mode which gives rise to the shear, these structural results suggest that an optic mode may also be involved in the transition. A full analysis of the possible optic modes which could couple to, or possibly drive, the soft acoustic mode is beyond the scope of this paper but will undoubtedly be the subject of future work.

## REFERENCES


1. G. R. Stewart, Z. Fisk and M. S. Wire, Phys. Rev. B 30, 482 (1984).
2. Y. Onuki, Y. Shimizu and T. Komatsubara, J. Phys. Soc. Japan 54, 470 (1985).
3. T. Shimizu, M. Takigawa, H. Yasuoka, Y. Onuki, and T. Komatsubara, J. Phys. Soc. Japan 54, 470 (1985).
4. D. T. Cromer, A. C. Larson, and R. B. Roof, Jr., Acta. Crystallogr. 13, 913, (1960).
5. J. D. Jorgensen and J. Faber, Jr., in "Proceedings of the Sixth Meeting of the International Collaboration on Advanced Neutron Sources," (Argonne National Laboratory, Report No. ANL-82-80, 1983) P. 105.
6. R. B. VonDreele, J. D. Jorgensen and C. G. Windsor, J. Appl. Crystallogr. 15, 581 (1982).
7. K. H. J. Buschow and A. S. van der Goot, J. Less-Common Metals 20, 309 (1970).

Table I. Structural Parameters of $CeCu_6$ vs Temperature. The structure is monoclinic, $P2_1/c$, for T = 10-200K and orthorhombic, Pmna, at 250K and 295K. Both space groups are expressed in the standard settings. $R_{wp}$ is the weighted profile value; $R_{exp}$ is the expected R value based on statistics.

| T(K) | a(A) | b(A) | c(A) | β(deg.) | V($A^3$) | $R_{wp}$ | $R_{exp}$ |
|---|---|---|---|---|---|---|---|
| 10 | 5.084(1) | 10.1279(2) | 8.0731(1) | 91.442(1) | 415.562(8) | 4.7084 | 2.6052 |
| 50 | 5.0861(1) | 10.1284(2) | 8.0740(1) | 91.341(1) | 415.811(8) | 4.8330 | 2.8529 |
| 100 | 5.0892(1) | 10.1326(2) | 8.0789(1) | 91.148(1) | 416.525(9) | 4.8346 | 2.6521 |
| 150 | 5.0921(1) | 10.1395(2) | 8.0860(2) | 90.896(2) | 417.443(9) | 5.0818 | 2.6963 |
| 175 | 5.0936(1) | 10.1428(2) | 8.0893(2) | 90.736(2) | 417.891(9) | 4.8858 | 2.6240 |
| 200 | 5.0950(1) | 10.1466(2) | 8.0931(2) | 90.485(2) | 418.376(10) | 5.0283 | 2.6494 |
| 250 | 8.1009(2) | 5.0978(1) | 10.1548(2) | | 419.358(11) | 5.8623 | 2.5979 |
| 295 | 8.1088(2) | 5.1004(1) | 10.1621(2) | | 420.286(12) | 5.8630 | 2.6218 |

Table II. Atomic positions and isotropic Debye-Waller factors of $CeCu_6$ at 295K in the orthorhombic Pnma space group and at 10K in the monoclinic $P2_1/c$ space group.

| 295K | | | | | 10 K | | | | |
|---|---|---|---|---|---|---|---|---|---|
| Atom | x | y | z | B | Atom | x | y | z | B |
| Ce | 0.2585(7) | 0.25 | 0.4364(6) | 0.789(1) | Ce | 0.2550(8) | 0.4363(4) | 0.2609(4) | 0.08(4) |
| Cu1 | 0.4350(2) | 0.0064(5) | 0.1901(3) | 0.680(1) | $Cu_1$ | 0.0070(9) | 0.1897(3) | 0.4363(3) | 0.13(4) |
| Cu2 | 0.1476(4) | 0.25 | 0.1432(3) | 0.812(1) | $Cu_2$ | 0.2454(5) | 0.1431(2) | 0.1462(3) | 0.12(3) |
| Cu3 | -0.1813(4) | 0.25 | -0.2454(3) | 0.698(1) | $Cu_3$ | 0.2520(5) | -0.2445(2) | -0.1813(3) | 0.07(3) |
| Cu4 | -0.4397(5) | 0.25 | -0.4038(3) | 1.119(1) | $Cu_4$ | 0.2278(5) | -0.4021(2) | -0.4382(3) | 0.02(4) |
| Cu5 | -0.1000(4) | 0.25 | -0.4836(3) | 0.780(1) | $Cu_5$ | 0.2495(5) | -0.4849(2) | -0.0998(3) | 0.21(4) |
| | | | | | $Cu_6$ | 0.5024(5) | -0.1917(3) | -0.4321(3) | 0.21(4) |

## FIGURE CAPTIONS

Figure 1: Portion of the raw time-of-flight neutron powder diffraction data (crosses) and best fit Rietveld least squares-fitted diffraction profile (solid line) for a monoclinic $P2_1/c$ model for $CeCu_6$ at 10K. Tick marks under the profile indicate the positions of all the allowed Bragg peaks. A difference plot (observed minus calculated intensity) appears at the bottom of plot. Background has been subtracted prior to plotting.

Figure 2: The square of the monoclinic strain (ac cos β) vs. temperature for $CeCu_6$. The straight line is a least-squares fit to the data.

Figure 3: Projection of the 10K structure of $CeCu_6$ along the monoclinic b axis. The straight lines at $x = 1/4$ and $3/4$ mark the planes in which all atoms except Cu1 are located in the high temperature orthorhombic structure.

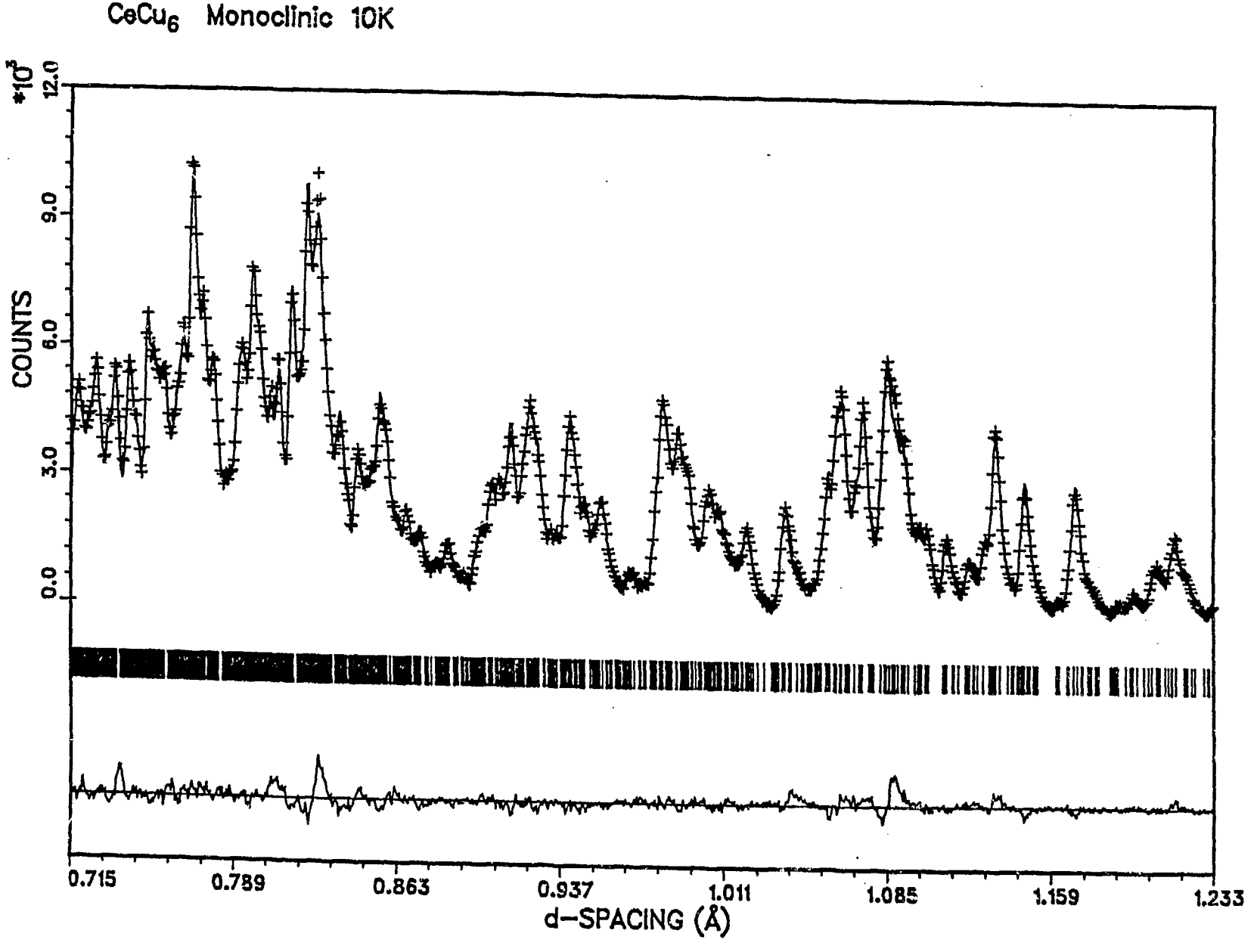
CeCu6 Monoclinic 10K
*10^3
12.0
9.0
6.0
3.0
0.0
COUNTS
0.715
0.789
0.863
0.937
1.011
1.085
1.159
1.233
d-SPACING (Å)

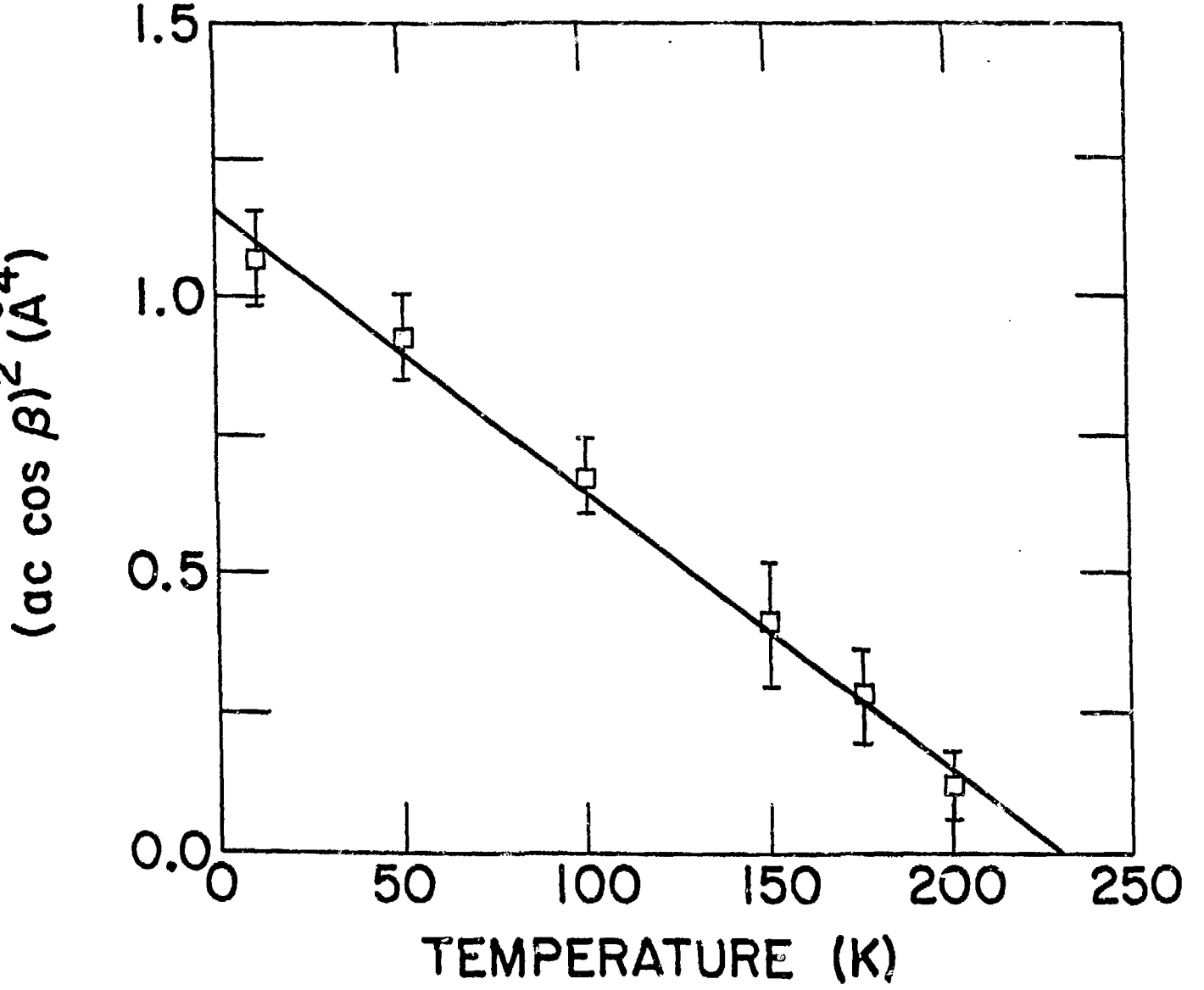
1.5
1.0
0.5
0.0
0
50
100
150
200
250
(ac cos β)² (Å⁴)
TEMPERATURE (K)

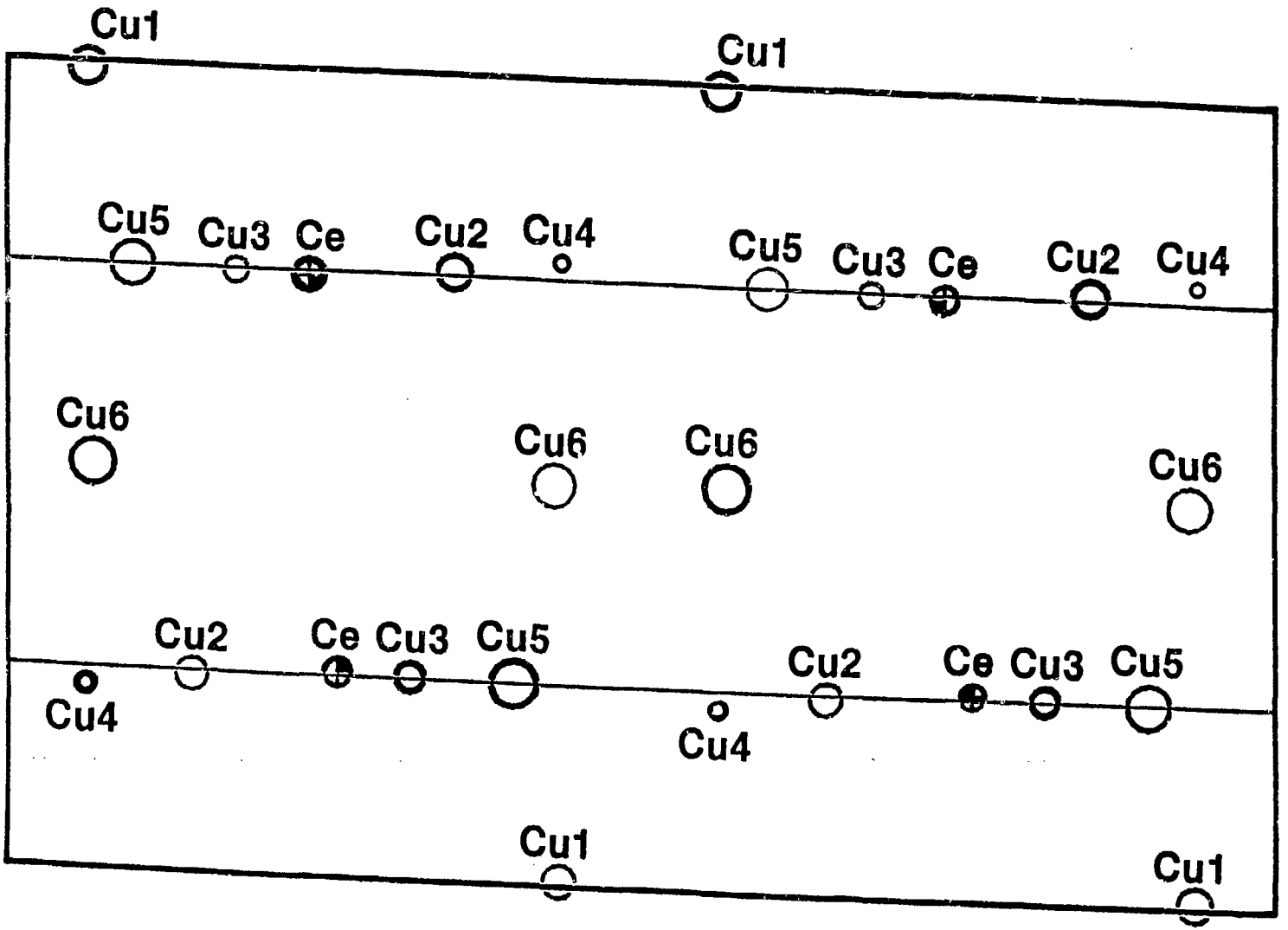
Cu1
Cu1
Cu5
Cu3
Ce
Cu2
Cu4
Cu5
Cu3
Ce
Cu2
Cu4
Cu6
Cu6
Cu6
Cu6
Cu2
Ce
Cu3
Cu5
Cu2
Ce
Cu3
Cu5
Cu4
Cu4
Cu1
Cu1